APPENDIX

Table of contents

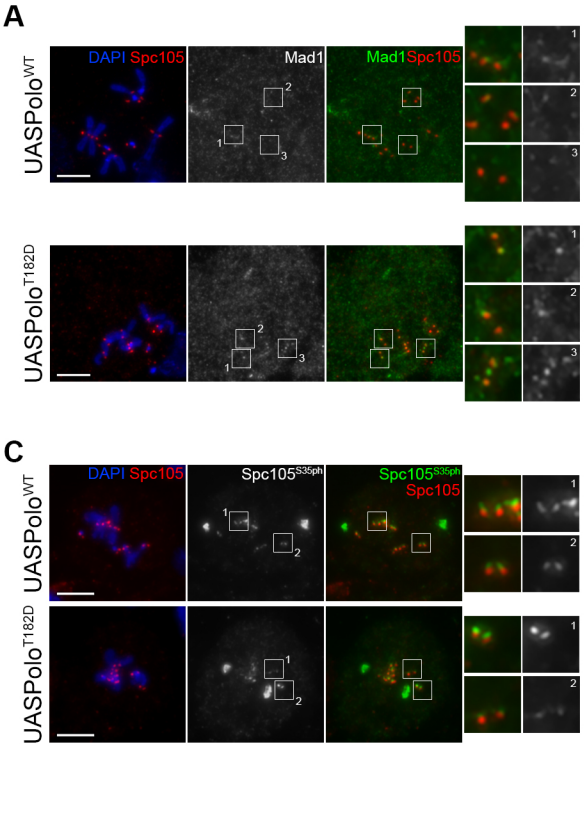

APPENDIX FIGURE S1

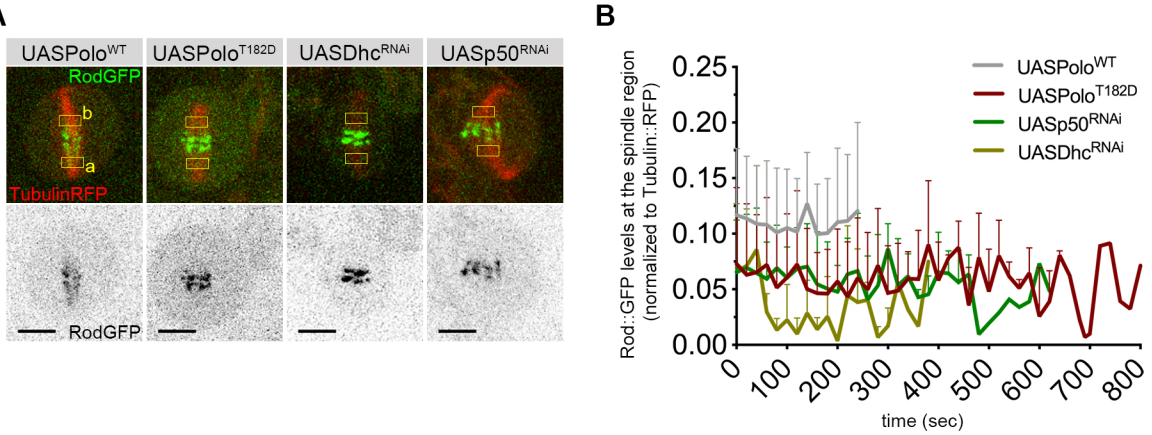

APPENDIX FIGURE S2

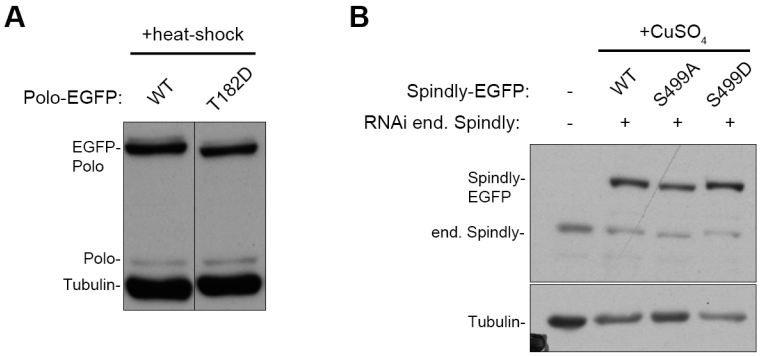

APPENDIX FIGURE S3

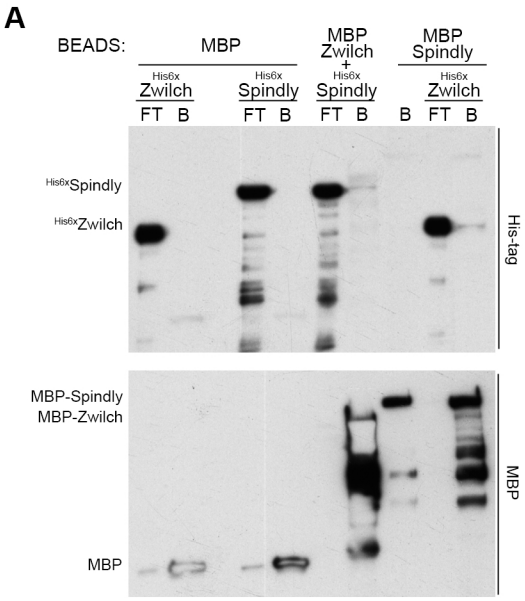

APPENDIX FIGURE S4

APPENDIX FIGURE LEGENDS

Appendix Figure S1. **Expression of Polo^{T182D} destabilizes KT-MT interactions but fails to significantly increase Aurora B activity**.

A) Representative immunofluorescence images of Mad1 localization at KTs of prometaphase *Drosophila* neuroblasts expressing either UAS-Polo^{WT} (used as control) or UAS-Polo^{T182}D. Insets show magnifications of the outlined regions which highlight increase number of KTs positive for Mad1. Spc105 was used as a KT reference.

(B) Graph represents the levels of Mad1 at KTs from prometaphase neuroblasts shown in (A). Mad1 signal was determined relative to Spc105 and all values were normalized to the control mean fluorescence intensity, which was set to 100% (n≥363 KTs from at least 30 neuroblasts for each condition, n=5 independent experiments).

(C) Representative immunofluorescence images of Spc105 phospho(ph)-S35 levels in unaligned KTs in neuroblasts expressing either UASPolo^{WT} (used as control) or UASPolo^{T182D}. Insets show magnifications of the outlined regions which highlight late congressing KTs.

(D) Graph represents the levels of Spc105phS35 at late congressing KTs for neuroblasts shown in (C). phS35 signal was determined relative to Spc105 and all values were normalized to the control mean fluorescence intensity, which was set to 100% (n≥61 KTs from at least 16 neuroblasts for each condition, n=4 independent experiments).

Data information: Statistical analysis was calculated using an unpaired t-test (Mann-Whitney). p values: ns, not significant; *, <0.05. Data are shown as mean ± SD. Scale bar: 5 μm.

Appendix Figure S2. **RZZ streaming along MTs depends on recruitment of Dynein to KTs and is reduced upon expression of Polo^{T182D}.**

(A) Selected stills from live imaging analysis of Rod-GFP streaming in neuroblasts expressing Polo^{WT}, Polo^{T182D}, or depleted of Dynactin subunit p50 (UASp50^{RNAi}) or Dynein heavy chain (UASDhc^{RNAi}). *a* and *b* regions of interest were used to determine the levels for Rod-GFP and Tubulin-RFP in each condition. Scale bar: 5 μm.

(B) Graph represents the mean fluorescence intensity (MFI) for Rod-GFP in the spindle regions identified as *a* and *b*. All values were normalized to Tubulin-RFP MFI to account for short variations in the focal plane (n≥3 neuroblasts for each condition; data for UASDhc^{RNAi} condition is from a single experiment). Data are shown as mean ± SD.

Appendix Figure S3. EGFP-tagged transgene expression levels in Drosophila S2 cells.

(A) Western blot analysis of EGFP-tagged Polo levels in Drosophila S2 cells shown in Fig.6A. Expression of EGFP-tagged Polo transgenes was induced using a heat-shock promoter. Tubulin was used as loading control.

(B) Western blot analysis of depletion efficiency for endogenous Spindly and of expression levels for RNAi-resistant Spindly^{WT}-EGFP, Spindly^{S499A}-EGFP and Spindly^{S499D}-EGFP transgenes. Drosophila S2 cells were exposed to $CuSO_4$ for induction of transgene expression. Tubulin was used as a loading control.

Appendix Figure S4. Spindly interacts with Zwilch *in vitro*.

(A) Western blot analysis of MBP-Zwilch or MBP-Spindly^{WT} pull down of his$_{6x}$-Spindly^{WT} or his$_{6x}$-Zwilch, respectively. Immobilized MBP was used as negative control. B:Beads, FT: Flow-through.

Appendix Table S1. List of the UAS-RNAi stocks used in the RNAi screen for Polo interactors

Gene	CG number	#stock (V-VDRC)		
Sas-4	CG10061	V106051		
CG10104	CG10104	V108431		
Nup98-96	CG10198	V109279		
SMC2	CG10212	V10711	V10713	V103406
nau	CG10250	V51311		
Rpt5	CG10370	V105133		
amos	CG10393	V100511		
RpS27	CG10423	V107108		
ko	CG10573	V31267		
Nak	CG10637	V109507		
vih	CG10682	V107720		
barr	CG10726	V26760	V26759	
dm	CG10798	V106066		
ida	CG10850	V108634		
lok	CG10895	V44981		
Klp67A	CG10923	V108852		
Prosalpha5	CG10938	V108380		
l(1)dd4	CG10988	V104667		
rdgB	CG11111	V6226		
Sirt7	CG11305	V18043		
nAcRbeta-64B	CG11348	V106570		
glu	CG11397	V10937		
fs(1)N	CG11411	V105859		
APC10	CG11419	V107331		
BtbVII	CG11494	V106063		
CG11596	CG11596	V108633		
Ubi-p63E	CG11624	V102379		
Nup358	CG11856	V38583		
Nup37	CG11875	V109814		
Rpn2	CG11888	V106457		

Prosbeta3	CG11981	V100561	
Prosbeta7	CG12000	V101990	
Det	CG12265	V105741	
pdm2	CG12287	V102126	
polo	CG12306	V20177	
Prosbeta5	CG12323	V107628	
Hsp83	CG1242	V108568	
pav	CG1258	V46137	
CG13330	CG13330	V18790	
CG13380	CG13380	V106112	
Rpt1	CG1341	V108834	
CG13623	CG13623	V17334	
SA-2	CG13916	V108267	
stg	CG1395	V17760	
Bsg25D	CG14025	V102527	
Bub1	CG14030	V101096	
CG14164	CG14164	V48827	
CG14215	CG14215	V103547	
Tao	CG14217	V107645	
CG14427	CG14427	V101827	
CG14442	CG14442	V107485	
APC7	CG14444	V17622	
Klp10A	CG1453	V41534	
Cp110	CG14617	V101161	
Cap-H2	CG14685	V24905	
Rpt6	CG1489	V100620	
Prosalpha7	CG1519	V102016	
CG1523	CG1523	V25199	
cathD	CG1548	V109651	
Kmn1	CG1558	V106889	V19530
mys	CG1560	V103704	
rod	CG1569	V19152	
CG15735	CG15735	V101762	
Pka-R2	CG15862	V101763	

dila	CG1625	V103788		
fzr2	CG16783	V32724		
Rpt3	CG16916	V100681		
skpA	CG16983	V107815		
CG17032	CG17032	V100337		
dod	CG17051	V25210		
Cep135	CG17081	V14195		
CG17134	CG17134	V100541		
Nek2	CG17256	V103408		
Prosalpha4T1	CG17268	V101203		
Pp2A-29B	CG17291	V49672		
Prosbeta4	CG17331	V19081		
Lk6	CG17342	V109663		
CG17493	CG17493	V40081		
mad2	CG17498	V106003		
gammaTub37C	CG17566	V109921		
Taf1	CG17603	V106119		
sw	CG18000	V101559		
Mis12	CG18156	V105052	V19098	V19097
spen	CG18497	V108828		
mtrm	CG18543	V107579		
lin19	CG1877	V108558		
CAP-D2	CG1911	V33424	V33423	
Acf1	CG1966	V33447		
dco	CG2048	V9241		
Mad1	CG2072	V43714		
Dfd	CG2189	V50110		
Rpt6R	CG2241	V105002		
Jra	CG2275	V107997		
TER94	CG2331	V24354		
Cdc23	CG2508	V107306		
Fs(2)Ket	CG2637	V107622		
rap	CG3000	V25553		
mus81	CG3026	V33688		

CG30382	CG30382	V21156	
SNF1A	CG3051	V106200	
mr	CG3060	V106986	
aur	CG3068	V108446	
14-3-3epsilon	CG31196	V108129	
CG31291	CG31291	V21308	
dpr17	CG31361	V100978	
Rbp9	CG3151	V101412	
gammaTub23C	CG3157	V107572	
CG31687	CG31687	V21393	
Cap-D3	CG31989	V29657	
CG32371	CG32371	V106233	
Myt1	CG32417	V105157	
chb	CG32435	V108620	
Smc5	CG32438	V38969	V38970
disco-r	CG32577	V101579	
Eb1	CG3265	V24451	
l(1)G0148	CG32742	V104902	
Sdic3	CG32823	V50764	
Nsf2	CG33101	V7743	
CG33277	CG33277	V108072	
Prosbeta2	CG3329	V103575	
p53	CG33336	V103001	
CG3342	CG3342	V40325	
CG3348	CG3348	V8690	
zormin	CG33484	V101304	
cana	CG33694	V49776	
cp309	CG33957	V101645	
slmb	CG3412	V107825	
Prosalpha4	CG3422	V105712	
SA	CG3423	V106046	
Rpt4	CG3455	V52663	
CycB	CG3510	V109611	
bi	CG3578	V100598	

mei-9	CG3697	V12670	
Grip84	CG3917	V105640	
Cep97	CG3980	V34774	
Prosbeta6	CG4097	V105673	
Mcm3	CG4206	V108214	
elav	CG4262	V37915	
CG42730	CG42730	V40858	
Pka-C1	CG4379	V101524	
fne	CG4396	V101508	
wee	CG4488	V106329	
smt3	CG4494	V105980	
Nup160	CG4738	V109318	
Tctp	CG4800	V45532	
cnn	CG4832	V110415	
RecQ5	CG4879	V13363	
CG4893	CG4893	V22358	
Prosalpha6	CG4904	V100703	
twe	CG4965	V104147	
msps	CG5000	V21982	
CG5004	CG5004	V26683	
CLIP-190	CG5020	V107176	
Doc1	CG5133	V104927	
Prosalpha2	CG5266	V29686	
CG5335	CG5335	V101295	
cdc2	CG5363	V106130	
Ote	CG5581	V105308	
CYLD	CG5603	V101414	
Prosalpha6T	CG5648	V35023	
Nup75	CG5733	V27495	
CG5790	CG5790	V45044	
CycB3	CG5814	V108009	
SMC1	CG6057	V108922	V6532
Tsc1	CG6147	V22252	
Grip75	CG6176	V106044	

Bruce	CG6303	V107620
DNApol-alpha180	CG6349	V103699
cmet	CG6392	V35081
CG6498	CG6498	V109282
Pp1alpha-96A	CG6593	V105525
BicD	CG6605	V108084
UbcD2	CG6720	V31158
Nup107	CG6743	V22407
Cdc16	CG6759	V103583
Sec13	CG6773	V50367
asp	CG6875	V2911
bora	CG6897	V35134
gig	CG6975	V103417
cdc14	CG7134	V103627
SAK	CG7186	V105102
Rpt4R	CG7257	V107551
eff	CG7425	V105731
Mcm2	CG7538	V103619
Bub3	CG7581	V21037
tap	CG7659	V46806
Nup43	CG7671	V108595
gwl	CG7719	V21046
Rpn1	CG7762	V103939
pic	CG7769	V108924
RpS8	CG7808	V106835
BubR1	CG7838	V26109
CG7911	CG7911	V102920
Nlp	CG7917	V22625
nudE	CG8104	V100713
pbl	CG8114	V109305
Dmn	CG8269	V23728
dmt	CG8374	V100550
Lis-1	CG8440	V106777
clu	CG8443	V100709

Kap-alpha1	CG8548	V108741		
Cdc27	CG8610	V35986		
Nup44A	CG8722	V106489		
CG9135	CG9135	V105403		
Pp1-13C	CG9156	V107770		
CG9170	CG9170	V108727		
shtd	CG9198	V29072		
Grip128	CG9201	V29074		
Gl	CG9206	V3785		
Prosalpha3	CG9327	V104373		
betaTub85D	CG9359	V109590		
alphaTub85E	CG9476	V103202		
Sdic1	CG9580	V50546		
if	CG9623	V100770		
nudC	CG9710	V104008		
CG9727	CG9727	V106182		
Cap	CG9802	V101501	V39205	V39207
CG9853	CG9853	V107346		
Prosbeta5R1	CG9868	V106943		
mit(1)15	CG9900	V108844		
Ndc80	CG9938	V29337		
RanGAP	CG9999	V108264		

Appendix Table S2. DroID-derived list of 222 genes predicted to be Polo interactors grouped according to broader Gene Ontology (GO) terms for biological processes

GO Term	Biological process	GO Term usage in gene list (%)
GO:0007049	cell cycle	46.76
GO:0048856	anatomical structure development	43.06
GO:0030154	cell differentiation	38.43
GO:0000278	mitotic cell cycle	35.65
GO:0000003	reproduction	34.26
GO:0022607	cellular component assembly	29.17
GO:0051276	chromosome organization	25.46
GO:0007010	cytoskeleton organization	25.00
GO:0006950	response to stress	24.07
GO:0034641	cellular nitrogen compound metabolic process	22.22
GO:0009056	catabolic process	21.76
GO:0140014	mitotic nuclear division	21.30
GO:0006464	cellular protein modification process	20.83
GO:0007059	chromosome segregation	19.91
GO:0007165	signal transduction	18.98
GO:0006810	transport	18.52
GO:0009058	biosynthetic process	18.06
GO:0009790	embryo development	13.89
GO:0048646	anatomical structure formation involved in morphogenesis	13.89
GO:0065003	macromolecular complex assembly	12.50
GO:0051301	cell division	12.50
GO:0000902	cell morphogenesis	11.11
GO:0040011	locomotion	9.72
GO:0006461	protein complex assembly	9.26
GO:0016192	vesicle-mediated transport	8.80
GO:0007267	cell-cell signaling	8.80
GO:0006259	DNA metabolic process	8.33
GO:0008283	cell proliferation	8.33
GO:0021700	developmental maturation	7.87
GO:0040007	growth	7.41
GO:0048870	cell motility	6.94
GO:0008219	cell death	6.94
GO:0042592	homeostatic process	5.56
GO:0006913	nucleocytoplasmic transport	5.56
GO:0050877	nervous system processs	5.09

GO:0002376	immune system process	5.09
GO:0044281	small molecule metabolic process	4.17
GO:0006914	autophagy	3.70
GO:0030705	cytoskeleton-dependent intracellular transport	3.70
GO:0005975	carbohydrate metabolic process	3.24
GO:0007568	aging	2.78
GO:0061024	membrane organization	2.78
GO:0006397	mRNA processing	1.85
GO:0007155	cell adhesion	1.39
GO:0006412	translation	1.39
GO:0006457	protein folding	0.93
GO:0006091	generation of precursor metabolites and energy	0.93
GO:0006629	lipid metabolic process	0.93
GO:0044403	symbiont process	0.93
GO:0051604	protein maturation	0.93
GO:0030198	extracellular matrix organization	0.46
GO:0032196	transposition	0.46
GO:0019748	secondary metabolic process	0.46
GO:0006790	sulfur compound metabolic process	0.46
GO:0042254	ribosome biogenesis	0.46
GO:0051186	cofactor metabolic process	0.46
GO:0034330	cell junction organization	0.46
GO:0043473	pigmentation	0.46
GO:0003013	circulatory system process	0.46
non-annotated	-	1.81

APPENDIX TABLE LEGENDS

Appendix Table S1. List of the UAS-RNAi stocks used in the RNAi screen for Polo interactors. UAS-RNAi lines ordered for the 222 candidate genes identified in DroID database (www.droidb.org) as putative Polo interactors. RNAi lines are highlighted in red when expression alone results in adult lethality. RNAi lines highlighted in yellow were not tested.

Appendix Table S2. DroID-derived list of 222 genes predicted to be Polo interactors grouped according to broader Gene Ontology (GO) terms for biological processes. List of GO terms for biological processes for the 222 candidate genes identified in DroID database (www.droidb.org) as putative Polo interactors. GO terms were ranked according to GO Term Mapper resource from go.princeton.edu.